Actual daily evapotranspiration and crop coefficients for an alpine meadow in the Qilian Mountains, northwest China

Yong Yang, Rensheng Chen, Yaoxuan Song, Chuntan Han, Jiufeng Liu and Zhangwen Liu

ABSTRACT

Actual daily evapotranspiration (ET_a) was measured in two weighing micro-lysimeters, from 1 July 2009 to 30 June 2011 on an alpine meadow in the Qilian Mountains, northwest China. The findings showed that the mean daily ET_a in the unfrozen and frozen periods was 2.0 mm and 0.2 mm, respectively. The dominant factor affecting ET_a in the unfrozen period was net radiation (*RN*), whereas those in the frozen period were soil surface temperature (T_s) and air temperature (T_a). The mean value of the daily crop coefficient (K_c) was 0.82 in the unfrozen period, and 0.19 in the frozen period. Regression analysis of K_c and the environmental variables indicated that T_a, T_s, relative humidity and soil surface water content (*SWC*), rather than *RN*, were the major factors influencing K_c throughout the whole measurement period and in the unfrozen period, although no clear correlative relationships were found between K_c and meteorological factors in the frozen period. Three daily empirical ET_a models for an alpine meadow were developed, also utilizing the FAO-56 Penman–Monteith approach to estimate reference evapotranspiration. They all exhibited good performances in the unfrozen period, but none were found suitable for the frozen period.

Key words | crop coefficient, evapotranspiration, micro-lysimeter, mountainous region

Yong Yang (corresponding author)
Rensheng Chen
Yaoxuan Song
Chuntan Han
Jiufeng Liu
Zhangwen Liu
Qilian Alpine Ecology and Hydrology Research Station, Key Laboratory of Ecohydrology Inland River Basin, Northwest Institute of Eco-Environment and Resources, Chinese Academy of Sciences,
Lanzhou 730000,
China
E-mail: *yy177@lzb.ac.cn*

INTRODUCTION

The majority of inland rivers in China, including the Heihe River, the Shiyang River, and the Shule River, originate from the Qilian Mountains, northwestern China, a huge mountain range on the northeastern Qinghai–Tibet Plateau (Dong *et al.* 2015). As a main water source conservation zone of northwest China (Sun & Liu 2013), the Qilian Mountains play a critical role in regional sustainable development, especially for the oasis belt in the arid Hexi Corridor (Dong *et al.* 2015). Under the influence of global warming, the rate of warming in high mountain regions is amplified with elevation (Mountain Research Initiative EDW Working Group 2015), and the temperature on the north slope of Qilian Mountains has increased by 0.29 °C/10a in the past 50 years (Li *et al.* 2012). As in other cold high mountain regions, warming has caused a series of changes in hydrological processes in the Qilian Mountains, including changes in glacier melt (Wu *et al.* 2015), seasonal snow cover (Bourque & Mir 2012), alpine permafrost distribution (Zhao *et al.* 2012), and runoff (Li *et al.* 2012), which have influenced the water resources of the mountains and the middle and downstreams area of inland rivers. However, evapotranspiration (ET), an integral part of the water cycle under cold high mountain conditions (Herrnegger *et al.* 2012), is still incompletely understood in the Qilian Mountains because of sparse observations and a lack of measured data (Kang *et al.* 2008).

In fact, measuring ET in cold high mountain regions poses a number of challenges. The low temperatures test the endurance of fieldworkers and their instruments, and

doi: 10.2166/nh.2016.124

Downloaded from https://iwaponline.com/hr/article-pdf/48/4/1131/365357/nh0481131.pdf
by guest

the distance of these areas from large urban centers raises the cost of logistics and reduces the availability of measured data (Woo 2008). The Bowen ratio–energy balance and eddy correlation methods are widely used to obtain actual evapotranspiration (ET_a) in a diversity of sites, but in cold alpine meadow regions, they are both time- and apparatus-consuming and applicable only when a number of requirements are fulfilled, and their assumption of spatial homogeneity is also frequently violated (Pauwels & Samson 2006). Micro-lysimeters offer a relatively cheap, robust and practical alternative for measuring ET_a, particularly for the high mountains (Zhang *et al.* 2003; Yang *et al.* 2013), where it is too expensive and difficult to build the large-scale weighing lysimeters. Although there are some limitations to the use of micro-lysimeters to estimate ET_a, such as the influence on ET_a of lysimeter length and surface soil moisture content, they have long been used for this purpose, and their reliability and modifications have been discussed by Lascano & van Bavel (1986) and Zhang *et al.* (2003). In sum, their low cost and ease of application renders micro-lysimeters appropriate for measuring ET_a on alpine meadows.

Owing to the difficulties of direct ET measurement in cold high mountain conditions, estimated methods provide an acceptable way of obtaining ET. As an analytical approach, the FAO-56 publication on crop ET_a (Allen *et al.* 1998) is the most widely used method worldwide (e.g., Sumner & Jacobs 2005; Pauwels & Samson 2006; Ngongondo *et al.* 2013; Reddy 2015). Ma *et al.* (2015b) proposed a complementary relationship method to simulate the ET in high-altitude regions. The FAO-56 method is commonly called the two-step approach, because it calculates the reference evapotranspiration (ET_0) first, and is then empirically adjusted using the crop coefficients (K_c) (Allen *et al.* 1998). Although the FAO-56 method has attracted criticism, it is a convenient way to estimate ET_a (Lhomme *et al.* 2015; Ma *et al.* 2015c). However, as an important adjustment ratio, K_c depends on the type and varieties of crops, crop height, leaf characteristics, soil properties, climate conditions, irrigation methods, and so on (Reddy 2015). Due to data limitations and for calculation simplification, Allen *et al.* (1998) suggest that K_c can be assumed to be a constant for a given vegetation growth stage, involving initial, crop development, mid-season and late season. Following the guidelines for computing ET_a (Allen *et al.* 1998), K_c can be simply estimated as a function of the green-leaf area index (*LAI*) (Sumner & Jacobs 2005), a regression function of air temperature (T_a), soil water content, relative humidity (*RH*), and *RN* (Zhou & Zhou 2009; Yang & Zhou 2011), or a polynomial function of sowing day (Reddy 2015). However, unlike the low altitude regions, because of a lack of ET_a measurements, there are few reports and/or discussions on K_c in high altitude mountainous regions.

The aims of this paper were to: (1) measure actual daily ET_a by micro-lysimeters, compare it with daily ET_0 from the FAO-56 Penman–Monteith (FPM) approach method; (2) investigate the factors influencing ET_a and K_c; and (3) develop a K_c and daily ET_a model on the basis of FPM ET_0 estimates for the application on an alpine meadow in the Qilian Mountains, northwest China.

STUDY SITE AND EXPERIMENTAL SETUP

The experiment was conducted at the Qilian Alpine Ecology & Hydrology Research Station (38°16′N, 99°52′E, altitude 2,980 m), which is located in the headwaters region of Heihe River in the Qilian Mountains (Figure 1). A standard meteorological observation field was built at the station on 20 June 2009, and an Environmental Information System (ENVIS, IMKO Micromodu1technik GmbH, Germany), was also installed to record half-hourly measurement of soil temperature (T8,

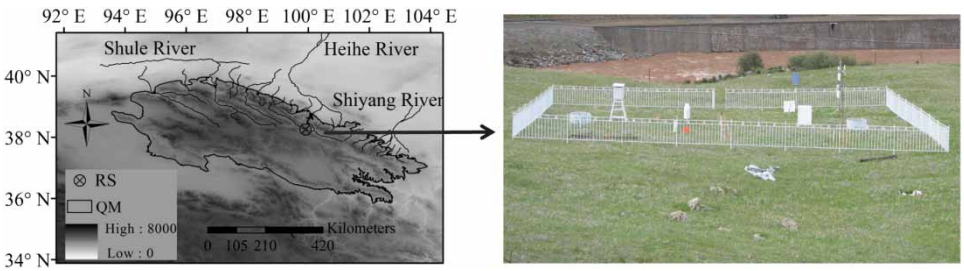

Figure 1 | Location and photograph of the meteorological observation in the Qilian Mountains (RS: research site; QM: Qilian Mountains).

Downloaded from https://iwaponline.com/hr/article-pdf/48/4/1131/365357/nh0481131.pdf
by guest

IMKO, Germany) and water contents at seven depths (0 cm for temperature/2 cm for water content, 20 cm, 40 cm, 60 cm, 80 cm, 120 cm and 160 cm, TRIME–EZ, IMKO, Germany), and a number of other meteorological variables, including solar radiation and reflected radiation (CMA6, Kipp & Zonen, the Netherlands), *RN* (Type 8110, Ph. Schenk GmbH Wien, Austria), precipitation (RG50, Seba Hydrometrie GmbH, Germany), soil heat flow (0.05 m, HFT-3, Campbell Scientific Ltd., USA), T_a and *RH* (HMP45D, Vaisala, Finland) at 1.5 m and 2.5 m, wind speed (*WS*) and direction (RITA Gray, IISA, Siggelkow Geratebau GmbH, Germany). According to meteorological data from the observation field and ENVIS, from 1 July 2009 to 30 June 2011, the mean T_a was approximately 1.5 °C in the observed period, with January and July averages of −8.6 °C and 14.5 °C, respectively. The mean annual *RH* and *RN* was 54.8% and 80.7 W m^{-2}, respectively. The mean annual precipitation over the two observation years was 446.9 mm, 90% of which occurred in the plant growing season (May to September). The research site was classified as seasonal frozen soil region, and the maximum frozen soil depth (*FSD*) was about 240 cm (Figure 2). The dominant species in the area were *Kobresia capillifolia* (Decne.) C.B. Clarke and *Carex moorcroftii* (Falc. ex Boott). The canopy cover was above 98%, and the vegetation root depth was nearly 35 cm.

Two lysimeters (labeled A and B) used in this study, of metal material, filled with a block of natural soil of the same size and shape as the drum, were installed by setting a cylindrical container into the soil at the level of the natural surface. Drawing from the useful research in similar localities (Zhang *et al.* 2003; Yang *et al.* 2013), the two lysimeters chosen for this work were both 40 cm in depth and 31.5 cm in diameter, to accommodate the depth of the majority of vegetation roots. The lysimeters were installed in the standard meteorological observation field, which was located in a flat pasture with representative vegetation and soil. Each was weighed daily at 20:00 (China Standard Time), with a balance of 2 g in precision, which corresponds to 0.026 mm. There are some limitations of micro-lysimeters in obtaining ET_a in an alpine environment. The lysimeter container could block the deep drainage, and the lysimeter material could influence the soil heat transfer. In this study, the designed length of the lysimeters was long enough to reduce the influences from deep soil water flow, and the metal material could transfer the heat well between

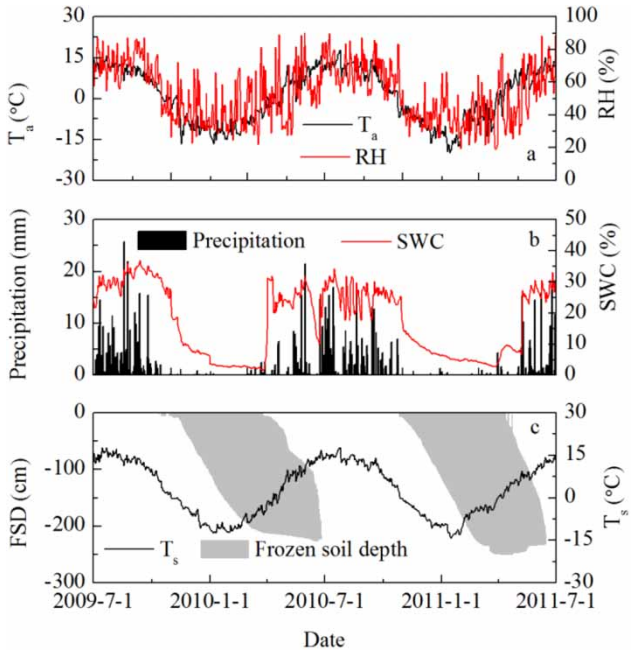

Figure 2 | Temporal variations of (a) daily air temperature (T_a) and *RH*, (b) daily precipitation and daily mean soil surface (2 cm) water content (*SWC*), (c) daily soil surface temperature (T_s) and *FSD* during the measurement period.

soils in and out of the lysimeters. There have been some successful field experiments with similar lysimeters in an alpine environment (Yang *et al.* 2013), so it was reasonable and acceptable to use the designed lysimeters to obtain ET_a at the research site. The micro-lysimeters were installed on 25 June 2009, with measurements taken from 1 July 2009 to 30 June 2011, to obtain the daily ET_a readings for the two consecutive years. Owing to the fact that soil freezes during the cold seasons in high-altitude mountainous regions, the measurement period was divided into unfrozen and frozen periods based on the measured soil surface temperature (T_s). Days on which T_s fell below 0 °C constituted the frozen period, and all other days were the unfrozen period.

METHODS

Measurement method

The weights of the lysimeters were measured every day, allowing ET_a to be calculated using the following equation:

$$ET_a = 10\Delta W/\rho S + P - 10I/\rho S \quad (1)$$

Downloaded from https://iwaponline.com/hr/article-pdf/48/4/1131/365357/nh0481131.pdf
by guest

where ET_a is the measured ET by the lysimeter method (mm day^{-1}); ΔW is the weight difference measured by the lysimeter (g day^{-1}); ρ is the water density (1 g cm^{-3}); S is the surface area of the soil within it (cm^2); P is precipitation (mm day^{-1}); and I is infiltration (g day^{-1}), measured by weighing daily, the same as the lysimeter.

FPM

The FPM method for calculating ET_0 (Allen *et al.* 1998) can be expressed as:

$$ET_0 = \frac{0.408\Delta(R_n - G) + \gamma \frac{900}{T_a + 273} u_2 (e_s - e_a)}{\Delta + \gamma(1 + 0.34u_2)} \quad (2)$$

where ET_0 is the reference ET estimated by FPM (mm day^{-1}); R_n is the RN at the grass surface (MJ m^{-2} day^{-1}); G is the soil heat flux (MJ m^{-2} day^{-1}); T_a is the average air temperature at 2 m height (°C); u_2 is the WS at 2 m height (m s^{-1}); e_s is the saturation vapor pressure (kPa); e_a is the actual vapor pressure (kPa); Δ is the slope of the saturated water vapor pressure curve (kPa °C^{-1}); and γ is the psychrometric constant (kPa °C^{-1}).

Crop coefficient

The crop coefficient (K_c), as an adjustment ratio, can be expressed as:

$$K_c = ET_a / ET_0 \quad (3)$$

where K_c is the crop coefficient, ET_a is from Equation (1), and ET_0 is from Equation (2).

Statistical analysis

Statistical indices were used for quantitative analysis of ET_a modeling performance. ET_a values measured by the lysimeters and computed through developed methods were compared by using a series of statistics. Errors were calculated as:

$$RMSE = \left[\frac{1}{n}\sum_{i=1}^{n}(E_i - M_i)^2\right]^{0.5} \quad (4)$$

$$MAD = \frac{1}{n}\sum_{i=1}^{n}|(E_i - M_i)| \quad (5)$$

$$R = \frac{\sum_{i=1}^{n}(E_i - \overline{E})(M_i - \overline{M})}{\sqrt{\sum_{i=1}^{n}(E_i - \overline{E})^2}\sqrt{\sum_{i=1}^{n}(M_i - \overline{M})^2}} \quad (6)$$

where RMSE, MAD, R, and R^2 are the root mean square error (mm day^{-1}), mean absolute deviation (mm day^{-1}), Pearson correlation coefficients, and coefficient of determination; n is the number of observation days; E_i are the estimated ET values (mm day^{-1}); M_i are ET values measured by the lysimeters (mm day^{-1}). The value of Pearson correlation coefficients is between 1 and −1 inclusively, where 1 is total positive correlation, 0 is no correlation, and −1 is total negative correlation. The regression functions and regression fitting lines in this study were directly provided by Origin 8.0 software.

RESULTS AND DISCUSSION

Determination of ET_a by lysimeters

Two micro-lysimeters were used to obtain an accurate determination of ET_a in an alpine meadow in the Qilian Mountains from 1 July 2009 to 30 June 2011. Figure 3 shows a comparison between the ET_a values recorded by lysimeter A and B. The values of the two lysimeters were in a very close range, and the average of the two lysimeters was taken as the actual daily ET on the research site. The total ET_a over the two years was 887.8 mm, 1.2 mm per day, accounting for 98.0% of precipitation during the experimental period. In the first year (from 1 July 2009 to 30 June 2010), the sum of ET_a was 451.5 mm, accounting for 99.1% of precipitation in the corresponding period. The figures for the second year (from 1 July 2010 to 30 June 2011) were 436.3 mm and 99.6%, respectively. The ratio of ET_a and precipitation showed that ET accounted for the largest loss of water cycle at the research site; another study reported a similar conclusion in a high altitude region (Ma *et al.* 2015a).

Obviously, seasonal variation in ET_a was observed at the research site (Figure 4), and the average daily ET_a in spring

Downloaded from https://iwaponline.com/hr/article-pdf/48/4/1131/365357/nh0481131.pdf
by guest

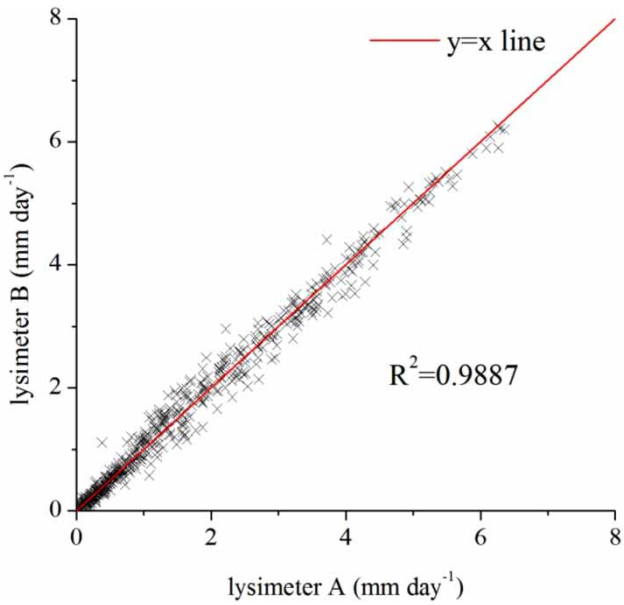

Figure 3 | Comparison between the measured ET_a from two micro-lysimeters.

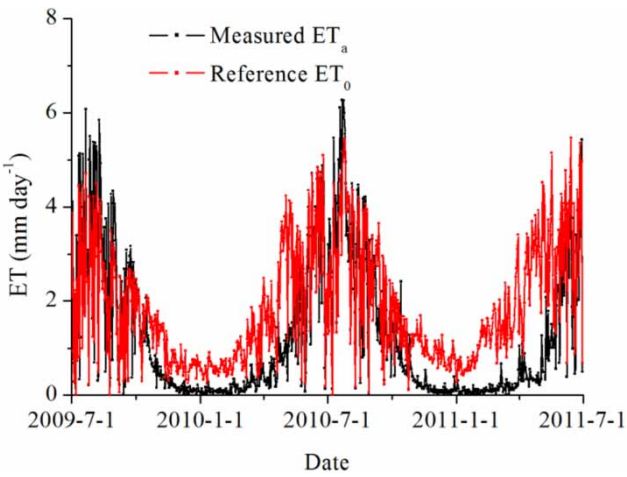

Figure 4 | Seasonal variations of daily measured ET_a and reference ET_0 during the measurement period.

(March–May), summer (June–August), autumn (September–November), and winter (December–February) was 0.7 mm, 3.1 mm, 1.0 mm, and 0.1 mm, respectively, and the daily reference ET_0 in four seasons was 2.2 mm, 2.9 mm, 2.0 mm, and 0.8 mm, respectively. The complicated and changeable weather in the alpine mountainous area led to short-term variations of the daily ET_a. The ET_a values in the frozen period were very small due to the low temperatures and frozen soil with little liquid water; and the bulk of ET_a occurred in the unfrozen period. The average daily ET_a in the frozen and unfrozen periods was 0.2 mm and 2.0 mm, respectively, and the reference ET_0 was 1.0 mm and 2.5 mm, respectively, in the two consecutive measured years. In the first year, the sum of ET_a in the unfrozen period (200 days) was 418.0 mm, accounting for 92.6% of ET_a in that year, whereas it was 411.7 mm in the second year (208 days), accounting for 94.4% of ET_a in that year.

Controlling factors affecting ET_a

The principal meteorological parameters affecting ET_a are radiation, T_a, RH, and WS (Allen *et al.* 1998). Water in the near surface soil is the source of ET_a. T_s was used to distinguish the frozen and unfrozen periods in this paper. Therefore, the influential meteorological factors discussed to control ET_a in this paper were RN ($W\,m^{-2}$), T_a (°C), T_s (°C), RH (%), WS ($m\,s^{-1}$), and SWC (%).

The Pearson correlation coefficients between ET_a and the meteorological factors were computed at daily scale (Table 1), with T_s, T_a, and RN found to be the most important factors in controlling ET_a throughout the whole measurement period, followed by SWC and RH. As most of the precipitation took place in the warm season on the research site, the SWC was close to saturation most of the time during the summer months (minimum of 22.5% and maximum of 35.5%, Figure 2). The land surface was wet or nearly wet in the unfrozen period, and the strong relationship between ET_a and RN indicated that the dominant factor affecting ET_a in this period was radiation, followed by T_s and T_a (Table 1). In the frozen period, in contrast, the plants grew very slowly and the frozen soil had very little liquid water content, roughly about 6% (Figure 2). The Pearson coefficients between ET_a and the meteorological parameters showed that ET_a was dominated by T_s and T_a in the frozen period, with RN and SWC exerting a similarly sized effect on ET_a. RH influenced ET_a over the entire measurement period, but its separate effects in the frozen and unfrozen periods could not be distinguished. WS was not a major control factor on ET_a in either period at the research sites.

The controlling factors that affect ET_a over different underlying surfaces in different climate regions are different; climate background, plant and soil type, and human

Downloaded from https://iwaponline.com/hr/article-pdf/48/4/1131/365357/nh0481131.pdf
by guest

Table 1 | Pearson correlation coefficients between actual evapotranspiration (ET_a) and meteorological variables of *RN*, air temperature (T_a), soil surface temperature (T_s), *RH*, *WS*, and soil surface water content (*SWC*) during the measurement period

Period	Factor	ET_a	*RN*	T_a	T_s	*RH*	*WS*	*SWC*
W	ET_a	1						
	RN	0.730**	1					
	T_a	0.736**	0.578**	1				
	T_s	0.752**	0.561**	0.971**	1			
	RH	0.430**	0.122**	0.608**	0.688**	1		
	WS	−0.165**	0.052	−0.061	−0.092*	−0.174**	1	
	SWC	0.617**	0.382**	0.785**	0.846**	0.691**	−0.171**	1
U	ET_a	1						
	RN	0.688**	1					
	T_a	0.601**	0.296**	1				
	T_s	0.651**	0.216**	0.898**	1			
	RH	0.059	−0.387**	0.231**	0.467**	1		
	WS	−0.209**	0.042	−0.155**	−0.271**	−0.304**	1	
	SWC	0.275**	−0.128**	0.160**	0.411**	0.552**	−0.330**	1
F	ET_a	1						
	RN	0.408**	1					
	T_a	0.487**	0.304**	1				
	T_s	0.572**	0.329**	0.824**	1			
	RH	0.139*	−0.134*	0.007	0.157**	1		
	WS	0.161**	0.238**	0.245**	0.280**	0.077	1	
	SWC	0.407**	0.035	0.445**	0.570**	0.122*	0.030	1

W: whole measured period, $n = 730$; U: unfrozen period, $n = 408$; F: frozen period, $n = 322$.
**$P < 0.01$; *$P < 0.05$.

interference can all be dominant factors. Over wet temperate grassland in Japan, *RN*, the atmospheric vapor pressure deficit, canopy surface conductance, and *LAI* all had an appreciable effect on ET_a measured via the eddy covariance technique (Li *et al.* 2005). Ryu *et al.* (2008) measured ET_a directly with the eddy covariance technique on a grassland in the Mediterranean climate zone of California, and found that monthly ET_a scaled negatively with solar radiation and was restrained by precipitation in the water-limited period; in the energy-limited period, on the other hand, the majority of ET_a scaled positively with solar radiation. In the temperate desert steppe in Inner Mongolia, China, ET_a measured via the eddy covariance method during the growing season showed *SWC* to be the dominant influential factor (Yang & Zhou 2011). In a study carried out in seven cropping zones in the Indus Basin in Pakistan, monthly ET_a estimated by the surface energy balance system was significantly controlled by mean T_a and rainfall, among several other climatological variables (e.g., *RN*, sunshine hours, and *WS*) (Liaqat *et al.* 2015).

K_c and its influence factors

In the current study, K_c, calculated based on Equation (3), displayed obvious daily and seasonal variations (Figure 5). The values of K_c were low in the frozen period, exhibited

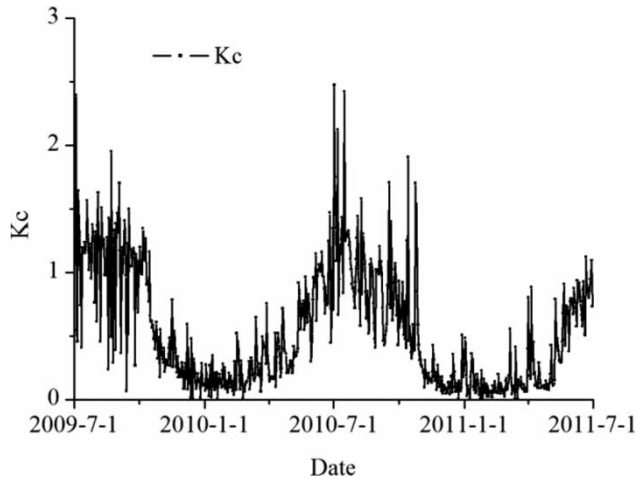

Figure 5 | Seasonal variations of daily K_c during the measurement period.

Downloaded from https://iwaponline.com/hr/article-pdf/48/4/1131/365357/nh0481131.pdf
by guest

a gradual rise from the frozen to the unfrozen period, and reached a peak in summertime, and then fell off as the frozen period approached. The daily K_c values ranged from 0.07 to 2.47 in the unfrozen period, with a mean value of 0.82, and from 0.01 to 0.79 in the frozen period, with a mean value of 0.19. Due to differences in climate background and plant type, K_c values in this study varied to a greater extent than those in studies carried out in other regions. K_c for reed marsh areas in the Liaohe Delta, Northeast China, ranged from 0.2 to 1.4, with a mean value of 0.53 in 2005 (Zhou & Zhou 2009). Migliaccio & Shoemaker (2014) reported monthly K_c values ranging from 0.62 to 0.92 for non-irrigated bahiagrass in subtropical south Florida, from May 2010 to January 2013.

It has long been known that climate exerts a major influence on K_c, which varies due to many meteorological factors, such as cloudiness, radiation, *WS*, temperature, and so on (Zhou & Zhou 2009). In this study, regression analysis was conducted between K_c and a number of environmental variables, namely, T_a, T_s, *RN*, *RH*, and *SWC*. Figure 6 and Table 2 show that T_a, T_s, *RH*, and *SWC*, but not *RN*, were the major factors influencing K_c throughout the whole measurement period and the unfrozen period. However, there were no clear correlative relationships between K_c and any of the meteorological factors in the frozen period. During that period, very little liquid water was available in the soil for evaporation, and there was almost no transpiration because of extremely limited plant activity. The FPM method, which was developed to calculate ET_0 with actively green grass growing and adequately watered (Allen *et al.* 1998), may not be suitable for the meteorological conditions that prevail in the frozen period on high altitude mountainous regions. This may explain the lack of clear statistical relationship between K_c and the meteorological factors in the frozen period.

K_c and ET_a models

Several studies of K_c model have been conducted. Sumner & Jacobs (2005) reported that K_c in a non-irrigated pasture site in Florida, USA, was a simple function of *LAI*. Zhou & Zhou (2009) reported that the daily K_c in a reed marsh in the Liaohe Delta, Northeast China, could be a function of *RN*, T_a, and *RH*. As there were no continuous *LAI* measurement data on the research site, and T_a, T_s, *RH*, and *SWC* were the major factors influencing K_c over the entire measurement period, the estimated daily K_c can be obtained from the equation empirically from the correlations and regression analysis between K_c and its major environmental controls:

$$K_{ce} = a \times T_a^2 + b \times T_a + c \times \exp(d \times RH) + e \times \exp(f \times SWC) + g \quad (7)$$

$$K_{ce} = a \times T_s^2 + b \times T_s + c \times \exp(d \times RH) + e \times \exp(f \times SWC) + g \quad (8)$$

where K_{ce} is estimated K_c; T_a and T_s are the air and soil surface temperature (°C); *RH* is relative humidity (%); and *SWC* is soil surface liquid water content (%); and a, b, c, d, e, f, and g are the parameters estimated through the regression.

In the Rajendranagar region of Andhra Pradesh in India, Reddy (2015) built a model for castor and maize crops, in which K_c was derived as a polynomial function of the number of days after sowing. Based on the good relationship between K_c and day of year (*DOY*) over the entire measurement period on the research site (Figure 6, Table 2), the estimated daily K_c can be given by the following equation:

$$K_{ce} = a \times D^3 + b \times D^2 + c \times D + d \quad (9)$$

where D is *DOY*; and a, b, c, and d are parameters estimated through the regression.

As the measurement period was two consecutive years, the data from the first year (from 1 July 2009 to 30 June 2010) were used to calibrate the regression coefficients in the K_c models (Equations (7)–(9)), and the data from the second year (from 1 July 2010 to 30 June 2011) were then used to validate the ET models. Based on daily meteorological data and ET_a in the first year, three empirical daily ET models for alpine meadow in the Qilian Mountains were developed:

$$ET_{ae} = (0.0016T_a^2 + 0.0237T_a + 14.6631\exp(0.0003RH) + 0.0506\exp(0.0602SWC) - 14.631)ET_0 \quad (10)$$

Downloaded from https://iwaponline.com/hr/article-pdf/48/4/1131/365357/nh0481131.pdf
by guest

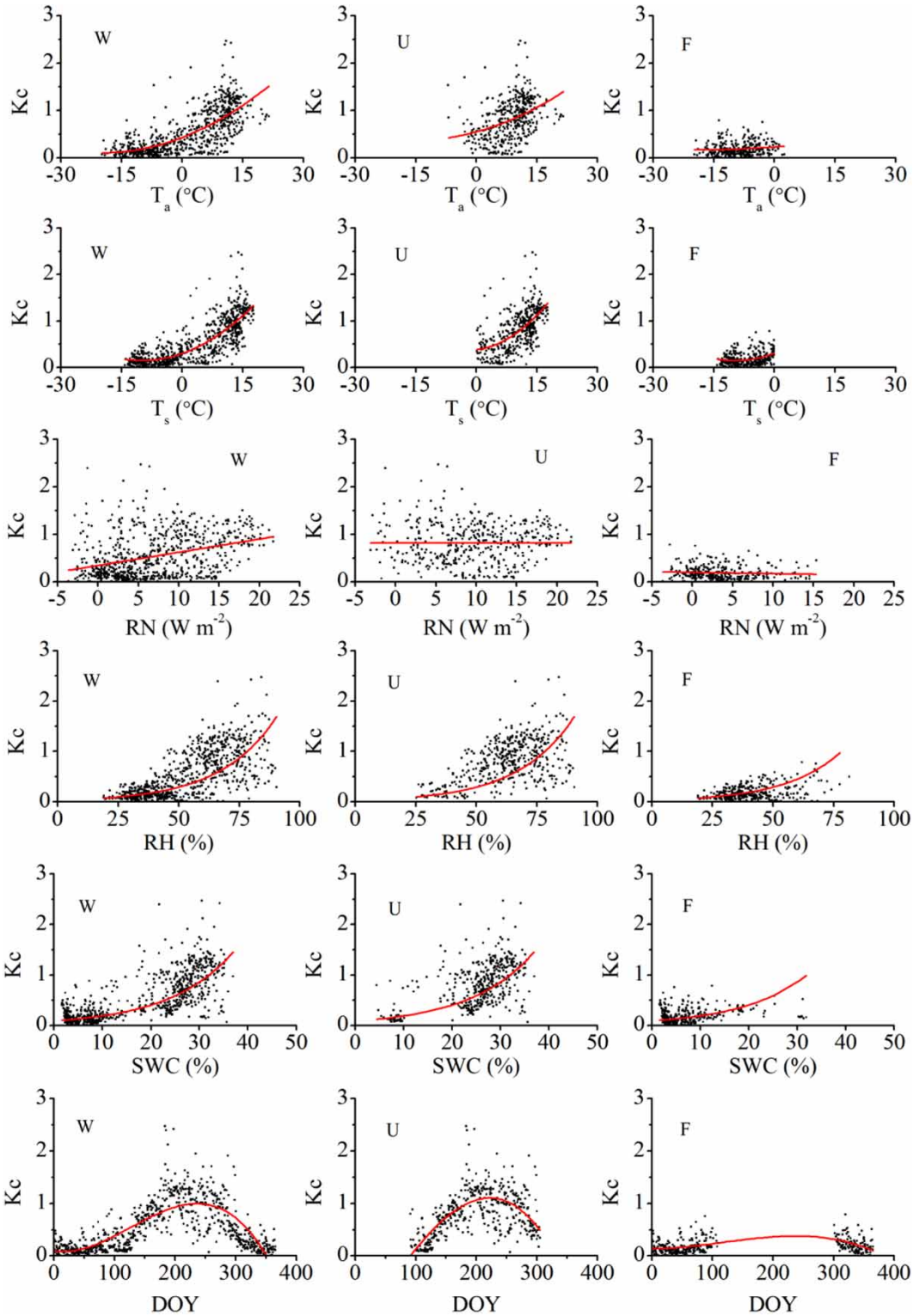

Figure 6 | Regression fitting lines between crop coefficients (K_c) and meteorological variables: air temperature (T_a), soil surface temperature (T_s), *RN*, *RH*, soil surface water content (*SWC*), and *DOY* in different measured periods (W: whole measurement period; U: unfrozen period; F: frozen period).

Downloaded from https://iwaponline.com/hr/article-pdf/48/4/1131/365357/nh0481131.pdf
by guest

Table 2 | Regression functions and coefficient of determinations (R^2) of crop coefficients (K_c) against several meteorological variables: air temperature (T_a), soil surface temperature (T_s), *RN*, *RH*, *WS*, soil surface water content (*SWC*), and *DOY*

Variables	Whole period	Unfrozen period	Frozen period
T_a	$y = 0.0008x^2 + 0.0328x + 0.4321$; $R^2 = 0.5264$	$y = 0.0007x^2 + 0.0233x + 0.5477$; $R^2 = 0.1573$	$y = 0.0002x^2 + 0.0064x + 0.2271$; $R^2 = 0.0125$
T_s	$y = 0.0015x^2 + 0.0308x + 0.3029$; $R^2 = 0.6552$	$y = 0.0026x^2 + 0.0096x + 0.3844$; $R^2 = 0.3688$	$y = 0.0017x^2 + 0.0330x + 0.3071$; $R^2 = 0.1204$
RN	$y = 0.0278x + 0.3451$; $R^2 = 0.1229$	$y = -0.00001x + 0.8164$; $R^2 = 2E\text{-}06$	$y = -0.0025x + 0.1977$; $R^2 = 0.0050$
RH	$y = 0.0334e^{0.0434x}$; $R^2 = 0.4451$	$y = 0.1143e^{0.0282x}$; $R^2 = 0.3398$	$y = 0.0738e^{0.0155x}$; $R^2 = 0.0410$
SWC	$y = 0.0898e^{0.0754x}$; $R^2 = 0.575$	$y = 0.1323e^{0.0639x}$; $R^2 = 0.4015$	$y = 0.1059e^{0.0373x}$; $R^2 = 0.0670$
DOY	$y = -2E\text{-}07x^3 + 6E\text{-}05x^2 - 0.0019x + 0.0946$; $R^2 = 0.5997$	$y = -1E\text{-}07x^3 - 4E\text{-}07x^2 + 0.0179x - 1.5438$; $R^2 = 0.4248$	$y = -3E\text{-}08x^3 + 1E-05x^2 + 0.0001x + 0.1311$; $R^2 = 0.1448$

$$ET_{ae} = (0.0012T_s^2 + 0.0255T_s + 8.6151\exp(0.0002RH) + 0.0061\exp(0.1001SWC) - 8.3838)ET_0 \quad (11)$$

$$ET_{ae} = (-0.0000002D^3 + 0.00008D^2 - 0.0016D + 0.1107)ET_0 \quad (12)$$

where ET_{ae} is estimated ET_a (mm day^{-1}), and ET_0 is the reference ET estimated by Equation (2) (mm day^{-1}).

The three models were tested using ET_a data collected during the measurement period. The slope of regression line (0.87) between the estimated (Equation (10)) and measured ET was close to 1, with R^2 of 0.89, RMSE of 0.49 mm day^{-1}, and MAD of 0.32 mm day^{-1} in the calibration period, whereas the slope was 1.08, with R^2 of 0.83, RMSE of 0.79 mm day^{-1}, and MAD of 0.46 mm day^{-1} in the validation period. Equation (11) based on T_s, *RH*, and *SWC* achieved better performance, with the slope of the regression line of 0.94, R^2 of 0.88, RMSE of 0.55 mm day^{-1}, and MAD of 0.36 mm day^{-1} over the entire validation period. A possible reason for this result was that T_s, rather than T_a, was the key indicator parameter of the energy process on soil surface, and exerted a strong influence on both K_c and ET. Based on the relationship between K_c and *DOY*, Equation (12), although it displayed poorer performance than the two other models over the entire validation period, with a slope of 1.17, R^2 of 0.80, RMSE of 1.28 mm day^{-1}, and MAD of 0.96 mm day^{-1}, could be used when data were limited because of its minimal input needs.

Scatter plots (Figure 7) and statistical analysis (Table 3) of the estimated and measured ET show that the three empirical daily ET models were able to calculate ET well for the unfrozen period, but were found to be unsuitable for the frozen period. The R^2 of estimated ET from Equations (10)–(12) against ET_a in the frozen validation period were 0.25, 0.25, and 0.23, respectively. The values of RMSE were 0.13 mm day^{-1}, 0.17 mm day^{-1}, 0.66 mm day^{-1}, respectively, and MAD were 0.10 mm day^{-1}, 0.13 mm day^{-1}, and 0.47 mm day^{-1}, respectively, whereas the mean daily ET_a in the frozen period was 0.2 mm day^{-1}. The assumptions of K_c and ET models, built to estimate crop ET with active green grass growth and adequate water in the low-altitude regions, might not be suitable for the actual growing and meteorological conditions in a high-altitude mountainous region during the winter months in which the ground was frozen. ET_a in the frozen period was very low, and potential measurement errors would be relatively large. The measurement errors might be the other reason for poor performances of ET_a models in the frozen period. Building a simple empirical daily K_c or ET model using meteorological variables might prove difficult in periods of freeze, because there was no clear relationship between those variables and K_c in the frozen period.

CONCLUSIONS

On an alpine meadow site located in the high Qilian Mountains, the total ET_a measured from micro-lysimeters, from 1 July 2009 to 30 June 2011, was 887.8 mm, 1.2 mm per day. The total ET_a was 451.5 mm in the first year (from 1 July

Downloaded from https://iwaponline.com/hr/article-pdf/48/4/1131/365357/nh0481131.pdf
by guest

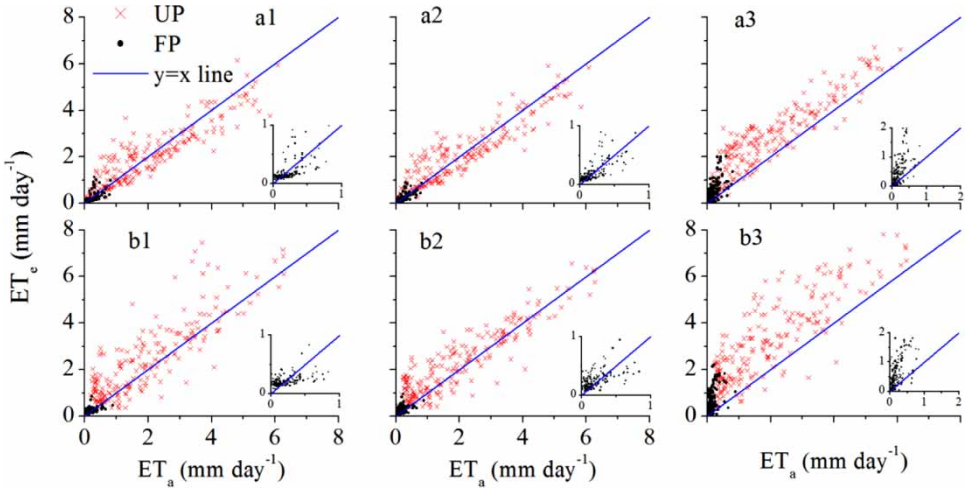

Figure 7 | Scatter plots of measured ET_a and estimated ET_e using Equations (10) (a1, b1), (11) (a2, b2), (12) (a3, b3) for the calibration period (a: from 1 July 2009 to 30 June 2010) and validation period (b: from 1 July 2010 to 30 June 2011). UP: cross scatter plots for measured and estimated ET in the unfrozen period; FP: dot scatter plots for measured and estimated ET in the frozen period.

Table 3 | Statistical analysis of evapotranspiration (ET_{ae}) estimates produced by the three empirical models compared with actual measured evapotranspiration (ET_a) (the former values for calibration period, from 1 July 2009 to 30 June 2010, and the latter for the validation period, from 1 July 2010 to 30 June 2011)

Model	Period	Slope	Intercept	R^2	RMSE (mm day^{-1})	MAD (mm day^{-1})
Equation (10)	W	0.87/1.08	0.16/0.21	0.89/0.83	0.49/0.79	0.32/0.46
	U	0.79/0.98	0.43/0.51	0.82/0.73	0.64/1.04	0.49/0.73
	F	0.73/0.36	0.06/0.16	0.37/0.25	0.16/0.13	0.10/0.10
Equation (11)	W	0.89/0.94	0.14/0.27	0.90/0.88	0.45/0.55	0.29/0.36
	U	0.82/0.85	0.39/0.58	0.84/0.81	0.60/0.72	0.46/0.55
	F	0.74/0.55	0.06/0.16	0.51/0.25	0.13/0.17	0.09/0.13
Equation (12)	W	1.08/1.17	0.47/0.72	0.88/0.80	0.82/1.28	0.60/0.96
	U	0.94/0.99	0.94/1.28	0.83/0.71	1.02/1.60	0.84/1.33
	F	1.74/1.90	0.13/0.32	0.39/0.23	0.48/0.66	0.31/0.47

W: whole measurement period; U: unfrozen period; F: frozen period[a].
[a]$ET_{ae} = \text{Slope} \times ET_a + \text{Intercept}$.

2009 to 30 June 2010), and 436.3 mm in the second. The ratio of ET to precipitation in the measurement period showed that ET was the main cause of water loss at the research site. Seasonal variations were found in the measured ET_a in the high-mountain regions, with the mean daily ET_a in the unfrozen and frozen periods measuring 2.0 and 0.2 per day, respectively. The dominant factor affecting ET_a in the unfrozen period was *RN*, whereas it was T_s and T_a in the frozen period.

The crop coefficient (K_c) for the alpine meadow in the high mountains showed obvious daily and seasonal variations, with daily K_c ranging from 0.07 to 2.47 in the unfrozen period, with a mean value of 0.82, and from 0.01 to 0.79 in the frozen period, with a mean value of 0.19. T_a, T_s, *RH*, and *SWC*, but not *RN*, were the major factors of influence for K_c over the whole measurement period and during the unfrozen period, but there were no clear correlative relationships between K_c and these meteorological factors in the frozen period.

Three daily K_c models were constructed. The first one was a function of T_a, *RH*, and *SWC*, while the second one was a function of T_s, *RH*, and *SWC*. The third K_c model was a polynomial function of *DOY*. Then, three empirical daily ET_a models derived from the FPM method were

Downloaded from https://iwaponline.com/hr/article-pdf/48/4/1131/365357/nh0481131.pdf
by guest

developed on the basis of those K_c models. The results indicated that the ET_a model based on T_s, RH, and SWC offered the best performance, with the slope of the regression line of 0.94, R^2 of 0.88, RMSE of 0.55 mm day^{-1}, and MAD of 0.36 mm day^{-1} for the whole validation period, and slope, R^2, RMSE, and MAD was 0.85, 0.81, 0.72, mm day^{-1} and 0.55 mm day^{-1}, respectively for the unfrozen validation period; and 0.55, 0.25, 0.17 mm day^{-1}, and 0.13 mm day^{-1}, respectively, for the frozen validation period. The three empirical daily ET_a models performed well in calculating ET_a at the research site during the unfrozen period, but were not suitable for the frozen period. The probable reason was that K_c and ET_0 from the FPM method provided inappropriate assumption for the actual plant growing and meteorological conditions in the high-altitude mountainous regions during the frozen period.

It is difficult to achieve a true understanding of ET in high mountain areas, because direct measurements of ET_a in those regions are not easily obtained. The results from this study will advance the understanding of actual daily ET_a and the difference in control factors between frozen and unfrozen periods. The three empirical daily ET_a models provided in this paper can be used for accurate quantitative estimates of the sensitivity of alpine meadow to climate change in high-altitude mountainous regions.

ACKNOWLEDGEMENTS

This work was carried out with financial support from the National Basic Research Program of China (2013CBA01806) and the National Natural Sciences Foundation of China (41401041). We thank the four reviewers and the editor for their constructive comments that led to improvements in the manuscript.

REFERENCES

Allen, R. G., Pereira, L. S., Raes, D. & Smith, M. 1998 *Crop Evapotranspiration – Guidelines for Computing Crop Water Requirements*. FAO Irrigation and Drainage Paper 56, Rome, Italy.

Bourque, C. P. A. & Mir, M. A. 2012 Seasonal snow cover in the Qilian Mountains of Northwest China: its dependence on oasis seasonal evolution and lowland production of water vapour. *Journal of Hydrology* **454–455**, 141–151.

Dong, L., Zhang, M., Wang, S., Qiang, F., Zhu, X. & Ren, Z. 2015 The freezing level height in the Qilian Mountains, northeast Tibetan Plateau based on reanalysis data and observations, 1979–2012. *Quaternary International* **380–381**, 60–67.

Herrnegger, M., Nachtnebel, H. P. & Haiden, T. 2012 Evapotranspiration in high alpine catchments – an important part of the water balance! *Hydrology Research* **43** (4), 460–475.

Kang, E. S., Chen, R. S., Zhang, Z. H., Ji, X. B. & Jin, B. W. 2008 Some problems facing hydrological and ecological researches in the mountain watershed at the upper stream of an inland river basin (in Chinese with English abstract). *Advances in Earth Science* **23** (7), 675–681.

Lascano, R. J. & van Bavel, C. H. M. 1986 Simulation and measurement of evaporation from a bare soil. *Soil Science Society of America Journal* **50** (5), 1127–1133.

Lhomme, J. P., Boudhina, N., Masmoudi, M. M. & Chehbouni, A. 2015 Estimation of crop water requirements: extending the one-step approach to dual crop coefficients. *Hydrology and Earth System Sciences* **19** (7), 3287–3299.

Li, S. G., Lai, C. T., Lee, G., Shimoda, S., Yokoyama, T., Higuchi, A. & Oikawa, T. 2005 Evapotranspiration from a wet temperate grassland and its sensitivity to microenvironmental variables. *Hydrological Processes* **19** (2), 517–532.

Li, B., Chen, Y., Chen, Z. & Li, W. 2012 Trends in runoff versus climate change in typical rivers in the arid region of northwest China. *Quaternary International* **282**, 87–95.

Liaqat, U. W., Choi, M. & Awan, U. K. 2015 Spatio-temporal distribution of actual evapotranspiration in the Indus Basin Irrigation System. *Hydrological Processes* **29** (11), 2613–2627.

Ma, N., Zhang, Y., Guo, Y., Gao, H., Zhang, H. & Wang, Y. 2015a Environmental and biophysical controls on the evapotranspiration over the highest alpine steppe. *Journal of Hydrology* **529**, 980–992.

Ma, N., Zhang, Y., Szilagyi, J., Guo, Y., Zhai, J. & Gao, H. 2015b Evaluating the complementary relationship of evapotranspiration in the alpine steppe of the Tibetan Plateau. *Water Resources Research* **51**, 1069–1083.

Ma, N., Zhang, Y., Xu, C. Y. & Szilagyi, J. 2015c Modeling actual evapotranspiration with routine meteorological variables in the data-scarce region of the Tibetan Plateau: comparisons and implications. *Journal of Geophysical Research: Biogeosciences* **120**, 1638–1657.

Migliaccio, K. W. & Shoemaker, W. B. 2014 Estimation of urban subtropical bahiagrass (Paspalum notatum) evapotranspiration using crop coefficients and the eddy covariance method. *Hydrological Processes* **28** (15), 4487–4495.

Mountain Research Initiative EDW Working Group. 2015 Elevation-dependent warming in mountain regions of the world. *Nature Climate Change* **5**, 424–430.

Ngongondo, C., Xu, C. Y., Tallaksen, L. M. & Alemaw, B. 2013 Evaluation of the FAO Penman–Monteith, Priestley–Taylor

Downloaded from https://iwaponline.com/hr/article-pdf/48/4/1131/365357/nh0481131.pdf
by guest

and Hargreaves models for estimating reference evapotranspiration in southern Malawi. *Hydrology Research* **44** (4), 706–722.

Pauwels, R. N. V. & Samson, R. 2006 Comparison of different methods to measure and model actual evapotranspiration rates for a wet sloping grassland. *Agricultural Water Management* **82**, 1–24.

Reddy, K. C. 2015 Development of crop coefficient models of castor and maize crops. *European Journal of Agronomy* **69**, 59–62.

Ryu, Y., Baldocchi, D. D., Ma, S. & Hehn, T. 2008 Interannual variability of evapotranspiration and energy exchange over an annual grassland in California. *Journal of Geophysical Research* **113**, D09104.

Sumner, D. M. & Jacobs, J. M. 2005 Utility of Penman–Monteith, Priestley–Taylor, reference evapotranspiration, and pan evaporation methods to estimate pasture evapotranspiration. *Journal of Hydrology* **308**, 81–104.

Sun, J. & Liu, Y. 2013 Drought variations in the middle Qilian Mountains, northeast Tibetan Plateau, over the last 450 years as reconstructed from tree rings. *Dendrochronologia* **31** (4), 279–285.

Woo, M. 2008 *Cold Region Atmospheric and Hydrologic Studies, the Mackenzie GEWEX Experience, Volume 2: Hydrologic Processes*. Springer, Berlin, Heidelberg, New York.

Wu, F., Zhan, J., Wang, Z. & Zhang, Q. 2015 Streamflow variation due to glacier melting and climate change in upstream Heihe River Basin, Northwest China. *Physics and Chemistry of the Earth, Parts A/B/C* **79–82**, 11–19.

Yang, F. & Zhou, G. 2011 Characteristics and modeling of evapotranspiration over a temperate desert steppe in Inner Mongolia, China. *Journal of Hydrology* **396** (1–2), 139–147.

Yang, Y., Chen, R., Han, C. & Qing, W. 2013 Measurement and estimation of the summertime daily evapotranspiration on alpine meadow in the Qilian Mountains, northwest China. *Environmental Earth Sciences* **68**, 2253–2261.

Zhang, Y., Ohata, T., Ersi, K. & Tandong, Y. 2003 Observation and estimation of evaporation from the ground surface of the cryosphere in Eastern Asia. *Hydrological Processes* **17** (6), 1135–1147.

Zhao, S., Cheng, W., Zhou, C., Chen, X. & Chen, J. 2012 Simulation of decadal alpine permafrost distributions in the Qilian Mountains over past 50 years by using Logistic Regression Model. *Cold Regions Science and Technology* **73**, 32–40.

Zhou, L. & Zhou, G. 2009 Measurement and modelling of evapotranspiration over a reed (Phragmites australis) marsh in Northeast China. *Journal of Hydrology* **372** (1–4), 41–47.

First received 14 January 2016; accepted in revised form 11 June 2016. Available online 29 July 2016

Downloaded from https://iwaponline.com/hr/article-pdf/48/4/1131/365357/nh0481131.pdf
by guest